Computer Modeling in Engineering & Sciences
DOI:10.32604/cmes.2020.012091
Article

Tech Science Press

Thermal Analysis of MHD Non-Newtonian Nanofluids over a Porous Media

Asad Ejaz[1], Imran Abbas[1], Yasir Nawaz[1], Muhammad Shoaib Arif[1], Wasfi Shatanawi[2,3,4,*] and Javeria Nawaz Abbasi[5]

[1]Stochastic Analysis & Optimization Research Group, Department of Mathematics, Air University, Islamabad, 44000, Pakistan
[2]Department of Mathematics and General Sciences, Prince Sultan University, Riyadh, 11586, Saudi Arabia
[3]Department of Medical Research, China Medical University Hospital, China Medical University, Taichung, 40402, Taiwan
[4]Department of Mathematics, Hashemite University, Zarqa, 13116, Jordan
[5]Department of Mathematics, Comsats University, Islamabad, 44000, Pakistan
*Corresponding Author: Wasfi Shatanawi. Email: wshatanawi@psu.edu.sa
Received: 14 June 2020; Accepted: 07 September 2020

Abstract: In the present research, Tiwari and Das model are used for the impact of a magnetic field on non-Newtonian nanofluid flow in the presence of injection and suction. The PDEs are converted into ordinary differential equations (ODEs) using the similarity method. The obtained ordinary differential equations are solved numerically using shooting method along with RK-4. Part of the present study uses nanoparticles (NPs) like TiO_2 and Al_2O_3 and sodium carboxymethyl cellulose (CMC/water) is considered as a base fluid (BF). This study is conducted to find the influence of nanoparticles, Prandtl number, and magnetic field on velocity and temperature profile, however, the Nusselt number and coefficient of skin friction parameters are also presented in detail with the variation of nanoparticles and parameters. The obtained results of the present study are presented using MATLAB. In addition to these, some simulations of partial differential equations are also shown using software for graphing surface plots of velocity profile and streamlines along with surface plots and isothermal contours of the temperature profile.

Keywords: MHD; non-Newtonian; nanofluids; porous medium; similarity solution; Blasius flow

Nomenclature

A	Constant
c	Constant
C_p	Specific heat at constant pressure
f	Un-dimensional flux form
f_w	The constant value of transpiration
h	Coefficient of Convection
k^*	Thermal conductivity
Pr	Prandtl No.

This work is licensed under a Creative Commons Attribution 4.0 International License, which permits unrestricted use, distribution, and reproduction in any medium, provided the original work is properly cited.

N	Power law index
$\overline{T}$	Fluid Temp
U_∞	The velocity of the free stream
$\breve{u}$	Velocity vector in x-direction
$\breve{v}$	Velocity vector in the y-direction
x	Coordinate along with the sheet
y	Coordinate perpendicular to the sheet surface

Greek Symbols

α	Thermal diffusivity
η	Variable for similarity solution
μ	Dynamic viscosity
θ	Non dimensional temperature
$\overline{\psi}$	Stream function
υ	Kinematic viscosity coefficient
$\dddot{\sigma}$	Electrical conductivity
φ	Volume fraction

Subscripts

f	Fluids
nf	Nanofluids
s	Solids
∞	Ambient conditions

1 Introduction

Solving Partial differential equations associated with fluid flow problems are the most fascinating and challenging task to perform. Its analysis, in reality, is also a hard job. In recent years computational techniques, coupled with laboratory framework, give more insight to fluid flow problems. The industries have an increasing interest in a non-Newtonian branch of fluid flow with different boundary conditions along with very similar parameters [1]. Such a convection mechanism is studied by Sui et al. [2] by considering non-Newtonian fluids to solve heat transfer problems using boundary methodology. Jalil et al. [3] obtain the solution to boundary flow with the assumption of the plane having properties of the permeable stretching sheet. They focused on the computational solution of this problem and compared the results with the analytical solution by the similarity of the equations. Patil et al. [4] studied the flow problem of power-law by considering mixed convection heat transfer on a flat vertical plate. Such a phenomenon gives rise to chemical reactions coupled with radiation under the assumption of a darcy porous medium. Researchers like Suresh et al. [5] focused on horizontal flat permeable moving slip velocity with heat and mass transfer.

The term NFs was introduced by Choi, and these are suspensions of solids particles with a diameter ranging from 1 nm to 100 nm. NFs containing base fluids and NPs are considered as a subclass for heat transfer fluids. In NFs, nanoparticles used are generally made of nano-metals. NFs are sufficiently viscous, adequate steady, better wetting, scattering and spreading property on solid surfaces even for modest NPs fixation. Choi et al. [6] investigated the increasing thermal conductivity of fluids with NPs. In view of the non-uniform thermal conductivity, Jha et al. [7] examined thermal transfer from non-Newtonian pseudo-plastic fluids. In a heat source traveling sheet, Mahmoud [8] has studied the impact of slip velocity on NFs power law fluid. Gadson et al. [9] discussed the application and convective heat transfer of NFs. Lin et al. [10] explored radiation transfer from a non-Newtonian Pseudoplastic NFs over a flat plate and Marangoni convection heat. The non-Newtonian Nanofluids flowing on a sheet with heat generation and MHD boundary layer absorption were analyzed numerically by Ramesh et al. [11]. Madhu et al. [12] reviewed the flow of non-Newtonian nanofluids over a non-linear stretching sheet. Yazdi et al. [13] studied the numerical calculation of magnetoconvection non-Newtonian nanofluids slip from a porous surface.

The flow alongside a fixed horizontal shield in a fluid stream flowing at a constant rate is a classic fluid mechanics problem. Blasius addressed such a flow in 1908. In this problem, the free stream is generated by the fluid motion. A related situation occurs when the plate moves in still fluid at a constant velocity. This topic was first handled by Sakiadis (1961). Dai et al. [14] explained Sakiadis and Blasius flow in NFs through a permeable surface in the existence of heat flow under a convective surface boundary condition. Study-related to the magnetic field effect on the classical Sakiadis and Blasius flow of NFs was discussed Ahmed et al. [15] over an inclined shield. A numerical computation was presented by Gupta et al. [16] in NFs on the Sakiadis and Blasius problems under isothermal conditions. From the outcomes of this study, it was come to know that the heat transfer and fluid flow properties of NFs are affected by solid volume fraction. In 1908 Blasius [17] solved the classical problem for the first time and still, it is a field of current research. Characteristics like heat and flow transfer in NFs were studied by Narsu et al. [18] in the presence of thermal radiation.

MHD refers to the investigation of magnetic properties for the fluid having electrical conduction. MHD has a wide range of applications in various fields of engineering such as power generator, cooling of reactors, MHD accelerator, and design for heat exchange. Alfven was the first physicist who gave the idea of MHD fluid flow. He reported that an electromotive force is produced due to the random motion of each conducting liquid placed in a magnetic field, which produced current, this current gives rise to the mechanical forces due to which fluids change their state of motion. Such type of rearrangement established electromagnetic hydrodynamic relations. Narsu and Rushi Kumar have analyzed the unsteady, laminar, two-dimensional MHD radiated and chemically reacting flow of Blasius and Sakiadis in the account of variables conductivity. The theoretical investigation of the assorted convective boundary layer flow with magnetic field NFs over an inclined plate was investigated by Devi and Kumar, and this study was discussed in account of both Blasius and Sakiadis flow. Further, the transformed governing equations were solved numerically with the help of MATLAB. The unsteady, laminar, and natural convective MHD with Blasius and Sakiadis flows with the help of various variable conditions and properties. And explained heat transfer and analyzed the existence of a crosswise magnetic field, injection, and suction, taking into consideration Brownian motion [19–22]. Arif et al. [23] observed the MHD nanofluid flowing with a chemical reaction over the rotating disc. Maleki et al. [24] studied flow and heat transfer in non-Newtonian nanofluids over a porous medium. Mustafa et al. [25] have analyzed the numerical solution for radiative heat transfer in ferrofluids flow due to a rotating disk. The focus of Umavathi et al. [26] was on the flow and heat transfer of the nanofluid porous composite medium. The magnetic field effects on Blasius and Sakiadis flow of nanofluids through a sliding plate have been checked by Anjali Devi et al. [27]. Mahanthesh et al. [28] observed heat and mass transfer effects over a moving vertical plate on mixed convective fluid flow of chemically reacting nanofluid. Oztop et al. [29] observed the numerical study of natural convection in partially based rectangular enclosures filled with nanofluids.

2 Formulation

Take into account the flow of a non-Newtonian power-law fluid along with a horizontal porous plate with indicating the velocity components in the directions of x and y-axes respectively, where x is the coordinate along with the plate, and y is the coordinate vertical to the x-axis. Fig. 1 shows the graphical model and the coordinate structure. Stream velocity and ambient temperature are represented by respectively. CMC/water is used as the base fluid for a pseudo-plastic non-Newtonian NFs. Tiwari and Das formulated a model on Boussinesq boundary layer approximation based on the nanofluid equation by considering the classical Blasius flow of nano liquid, equation of motion and heat transfer is elaborated as follow:

$$\breve{u}_x + \breve{v}_y = 0, \tag{1}$$

$$\tilde{u}\frac{\partial \tilde{u}}{\partial x} + \tilde{v}\frac{\partial \tilde{u}}{\partial y} = \frac{\mu_{nf}}{\rho_{nf}}\frac{\partial}{\partial y}\left(\left|\frac{\partial \tilde{u}}{\partial y}\right|^{n-1}\frac{\partial \tilde{u}}{\partial y}\right) - \frac{\sigma_{nf} {B_0}^2}{\rho_{nf}}\left(\tilde{u}\right), \tag{2}$$

$$\tilde{u}\frac{\partial \tilde{T}}{\partial x} + \tilde{v}\frac{\partial \tilde{T}}{\partial y} = \alpha_{nf}\frac{\partial}{\partial y}\left(\left|\frac{\partial \widehat{T}}{\partial y}\right|^{n-1}\frac{\partial \tilde{T}}{\partial y}\right). \tag{3}$$

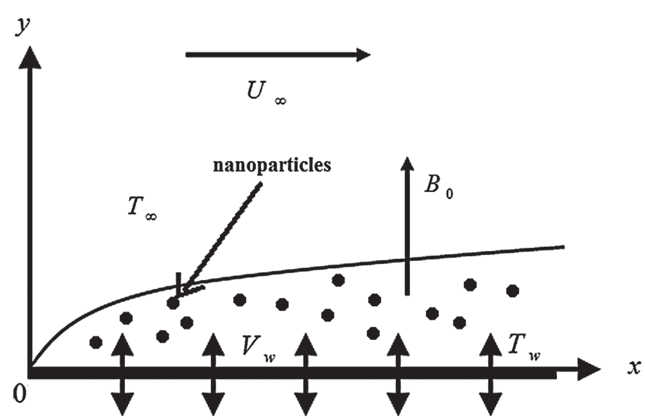

Figure 1: Geometry of fluid flow model

Boundary conditions are given as:

$$\breve{u} \to U_\infty \quad \text{as } y \to \infty,$$

$$\breve{u} = 0, \quad \breve{v} = V_w(x) \quad \text{at } y = 0. \tag{4}$$

$$-k_{nf}\frac{\partial \breve{T}}{\partial y} = h_f\left(T_f - T_w\right) \quad \text{at } y = 0,$$

$$\breve{T} \to T_\infty \quad \text{as } y \to \infty. \tag{5}$$

where $\tilde{\rho}_{nf}$, $\tilde{\alpha}_{nf}$ are respectively the density and thermal diffusivity of the nanofluids, $\breve{u}$ and $\breve{v}$ are the horizontal and vertical components of velocity in x and y directions respectively, and B_0 are taken as the strength of the magnetic field.

3 Thermo Physical Characteristic

The thermo physical characteristics of considered nanofluids are listed in Tab. 1 The comparison values of skin fraction for non-Newtonian case for selected values of transpiration are listed in Tab. 2. The comparison values of Nusselt number for non-Newtonian case for different values of Prandtl number are listed in Tab. 3.

The results in Tab. 1 laminar, incompressible flow regime is considered for the model in Tabs. 2 and 3 shows that our results are more efficient than the previous results which shows in the table.

Table 1: Thermophysical characteristics of Nps and base fluid [29]

Physical properties	CMC (0.0%–0.3%)	Cu	Al_2O_3	CuO	TiO_2
Cp	4179	385	765	535.6	686.2
Density	997.3	8933	3970	6500	4250
K^*	0.613	400	40	20	8.9538

Table 2: Comparison of the values of $f''(0)$ $n = 0.85$ and for various values f_w

f_w	Chen et al. [20]	Mostafa et al. [25]	Present results
0	−0.4438	−0.4437	−0.4436
0.1	−0.4737	−0.4736	−0.4735
0.5	−0.603	−0.602	−0.601
1	−0.7864	−0.7862	−0.7861

Table 3: Comparison of values $\theta'(0)$ for various values **Pr** when $f_w = 0$ and $n = 0.85$

Pr	Chen et al. [20]	Mostafa et al. [25]	Present results
0.7	0.3425	0.3423	0.342
1	0.44375	0.44372	0.44371
7	1.387	1.377	1.376
10	1.6802	1.68	1.6801

In the present discussion, NFs are used from [29] which are given as

$$\tilde{\alpha}_{nf} = \frac{k_{nf}}{(\rho C_p)_{nf}}, \quad \tilde{\mu}_{nf} = \frac{u}{(1-\varphi^{2.5})}, \quad \frac{k_{\mathrm{nf}}}{k_{\mathrm{f}}} = \frac{(k_s + 2k_f) - 2\varphi(k_f - k_s)}{(k_s + 2k_f) + \varphi(k_f - k_s)},$$

$$(\rho \mathrm{C_p})_{nf} = (1-\varphi)(\rho C_p)_f + \varphi(\rho C_p), \quad \tilde{\rho}_{nf} = (1-\varphi)\rho_{\mathrm{f}} + \varphi\rho_{\mathrm{s}}. \tag{6}$$

4 Solution Procedure

We use the following transformation laws for the conversion of governing equations into dimensionless form

$$\overline{\psi} = \left(U_\infty{}^{2n-1} \nu f_x\right)^{1/n+1} f(\eta), \quad \breve{u} = \overline{\psi}_y, \quad \breve{v} = -\overline{\psi}_x, \tag{7}$$

$$\breve{u} = U_\infty f(\eta), \quad \breve{v} = -\frac{1}{n+1}\left(\frac{\nu_f U\infty^{2n-1}}{x^n}\right)^{1/n+1}, \quad \eta = \left(\frac{U_\infty{}^{2-n}}{\nu_f x}\right)^{1/n+1} y, \quad \theta = \frac{\breve{T} - T_\infty}{T_{f-}T_\infty} \tag{8}$$

On applying boundary conditions the Blasius flow of the momentum and energy equations can be described as

$$\frac{1}{A_4 A_1}\left(\left|f''\right|^{n-1} f''\right)' + \frac{1}{n+1} f'' f - \overline{M}^2 \frac{\sigma_{nf}}{\sigma_f} f' = 0, \tag{9}$$

$$-\frac{A_3}{\mathrm{Pr}_f\, A_2}\left(|f''|^{n-1}\theta'\right)' + \frac{1}{n+1} f\theta' = 0. \tag{10}$$

where

$$\sigma_{nf} = (1-\varphi)\,\sigma_f + \varphi_s, \quad \overline{M} = \sqrt{\frac{B^2{}_0}{\tilde{\rho}_f}} \tag{11}$$

Boundary conditions are changed as follows

$$f(0) = f_w, \quad f'(0) = 0, \quad f'(\infty) = 1, \tag{12}$$

$$\theta'(0) = A_3 a\,(1 - \theta(0)), \quad \theta(\infty) = 0. \tag{13}$$

$fw = -1,\ 0,\ 1$ stands for impermeable sheet suction and injection respectively.

$$\left.\begin{aligned} A_1 &= \frac{1}{(1-\varphi) + \varphi\rho_s/\rho_f}, \quad A_2 = -\frac{1}{(1-\varphi) + \varphi\left(\rho C_p\right)_s / \left(\rho C_p\right)_f} \\ A_3 &= -\frac{\left(k_s/k_f + 2\right) - 2\varphi\left(1 - k_s/k_f\right)}{\left(k_s/k_f + 2\right) + \varphi\left(1 - k_s/k_f\right)}, \quad A_4 = \frac{1}{(1-\varphi)^{2.5}}. \end{aligned}\right\} \tag{14}$$

5 Quantities of Engineering Interest

The local skin friction coefficient C_f and the local Nusselt number Nu are quantities of physical interest and are defined in this paper as

$$C_{fx} = -2\tau_w/\rho_f U^2, \quad Nu_x = \frac{xq_w}{k_f\,(T_w - T\infty)} \tag{15}$$

By employing similarity variables in (15), the following forms are obtained.

$$\tau = \mu_{nf}\left(|u_y|^{n-1} u_y\right)_{y=0} \quad q_w = -k_{nf}\left(T_y\right)_{y=0} \quad \tilde{u} = U_\infty f'(\eta) \tag{16}$$

$$\tau_w = \frac{\partial u}{\partial y} = U_\infty \left({U_\infty}^{2-n} / v f_x \right) 1/\mathrm{n} + 1 f'' (\eta) \tag{17}$$

Putting values in Eq. (15) then following results are obtained

$$Cf_x {\mathrm{Re}_x}^{1/\mathrm{n}+1} = -2 \frac{\mu_{nf}}{\mu_f} f'' (0) \left| f'' (0) \right|^{n-1} \tag{18}$$

Similarly if we want to find Nusselt number we use Eq. (15) and the following temperature equation

$$\overline{T} = \left(T_f - T_\infty \right) \theta (\eta) + T_\infty \tag{19}$$

Differentiate Eq. (19) with respect to y following results are obtained

$$\frac{\partial \overline{T}}{\partial y} = \left(T_f - T_\infty \right) \theta' (\eta) \left({\mathrm{U}_\infty}^{2-n} / v f_x \right)^{1/n+1} \tag{20}$$

The following results can be obtained by the use of Eq. (20)

$$N_{ux} = \frac{x \left(k_{nf} \right) \left(T_f - T_\infty \right) \theta' \left({U_\infty}^{2-n} / v f_x \right)^{1/n+1}}{k_f \left(\mathrm{T}_w - T_\infty \right)} \tag{21}$$

After simplifying the above equation, the following results can be obtained

$$Nu_x {R_x}^{-1/n+1} = -\frac{k_{nf}}{k_f} \theta' (0) \quad \mathrm{Re_x} = \frac{U^{2-n} x^n}{v_f} \tag{22}$$

$$Cf_x {\mathrm{Re}_x}^{1/\mathrm{n}+1} = -2 \frac{\mu_{nf}}{\mu_f} f'' (0) \left| f'' (0) \right|^{n-1}, \quad Nu_x {\mathrm{Re}_x}^{-1/n+1} = -\frac{k_{nf}}{k_f} \theta' (0) . \tag{23}$$

6 Results and Discussions

The parameters used in a present study like Prandtl number and Nusselt number are defined below. Fig. 2 is drawn to explain the influence of Blasius flow on the velocity profile for the non-Newtonian case. It is clear from the diagram that the velocity profile is raising with increasing values of volume fraction.

Fig. 3 shows the relation between magnetic parameter M and the velocity profile for Blasius flow. The velocity profile is seemed to rise for bigger values of M for non-Newtonian fluids.

Fig. 4 is formed to investigate the effect of f_w on velocity profile for Blasius flow. When f_w increases, velocity profile, increases in the suction case, whereas reverse tendency is examined in the injection case.

Fig. 5 indicates that the suction parameter is increased when the temperature falls that is equivalent to saying faster cooling of the plate occurs with the greater suction which is essential for many applications in engineering even to waterproof and suction plate non-dimensional surface. While in injection case opposite trend is examined for both case TiO_2.

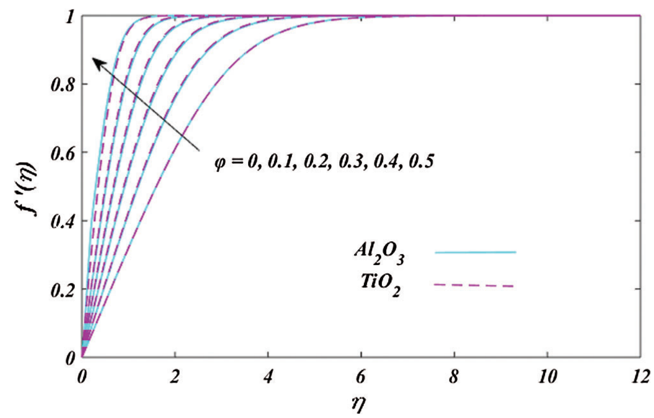

Figure 2: Effect of $f'(\eta)$ with φ

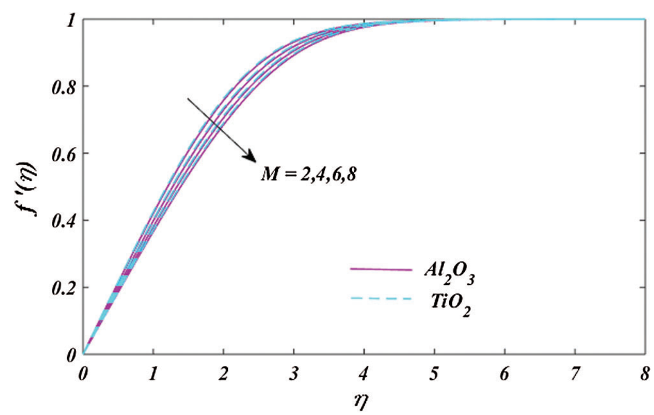

Figure 3: Effect of $f'(\eta)$ with magnetic parameter M

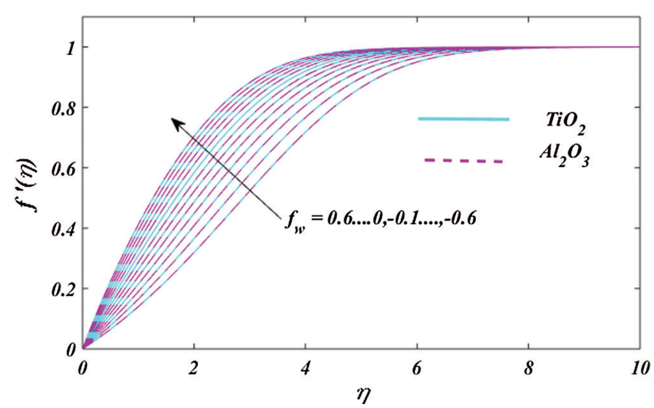

Figure 4: Effect of $f'(\eta)$ with f_w

Fig. 6 indicates that the suction parameter is increased when the temperature falls, which is essential for many applications in engineering. While in injection case opposite trend is shown for both cases Al_2O_3.

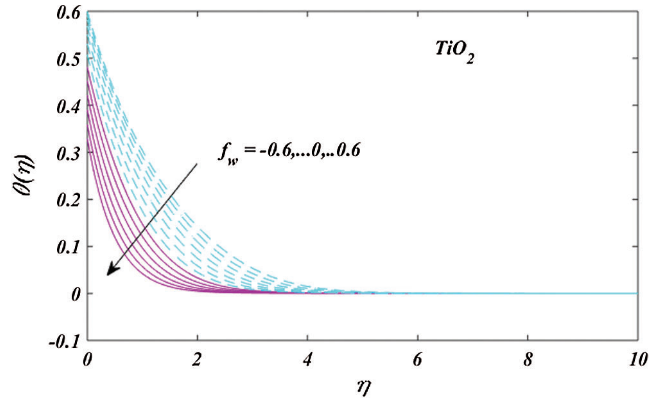

Figure 5: Effect of $\theta(\eta)$ with f_w

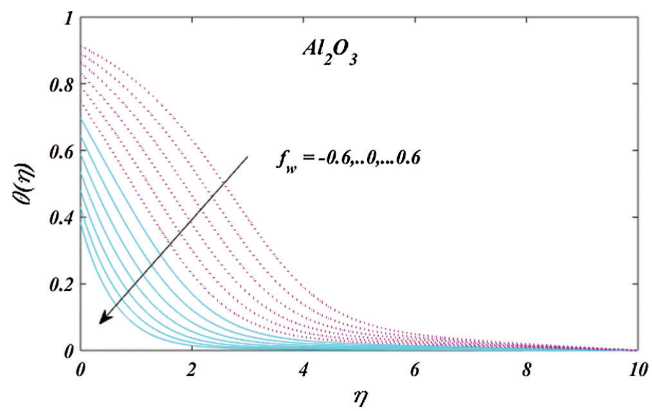

Figure 6: Effect of $\theta(\eta)$ with f_w

Fig. 7 shows the effect of volume fraction parameter on the temperature profiles. It is evident from the figure that rises in the volume fraction increases temperature profiles.

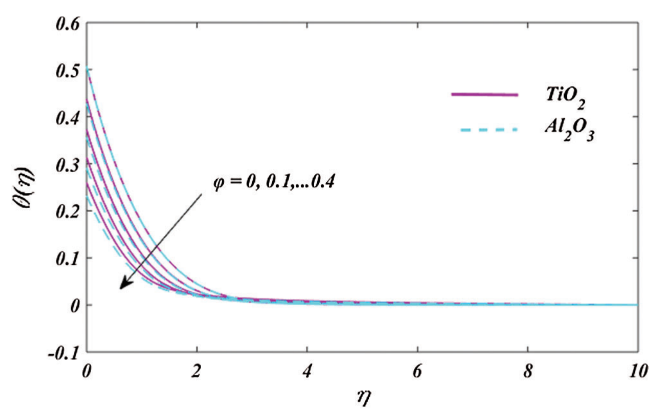

Figure 7: Effect of $\theta(\eta)$ with φ

Fig. 8 shows the impact of the Prandtl number on the temperature profile. From the figure, it is clear that an increase in the Prandtl number increases the temperature profile.

Fig. 9 shows the impact of magnetic field parameters. From the figure, it is clear that the increase in the magnetic field increases the temperature profile.

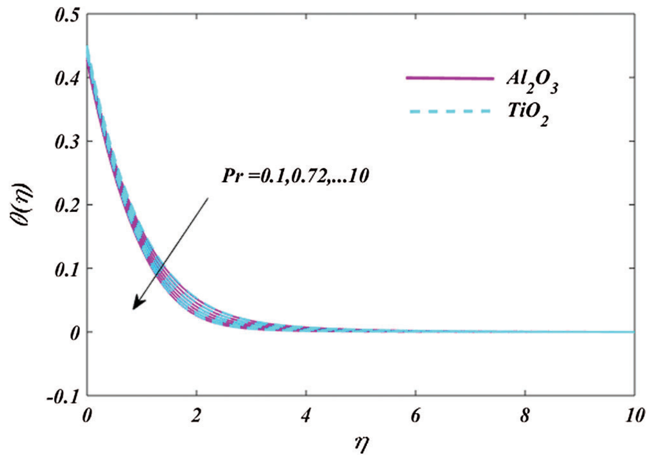

Figure 8: Effect of $\theta(\eta)$ with P

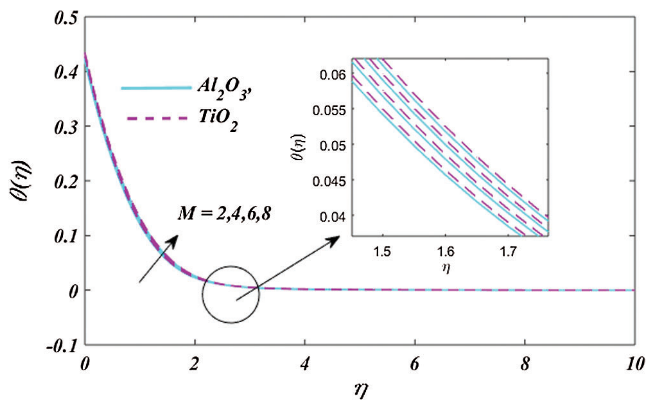

Figure 9: Effect of $\theta(\eta)$ with magnetic parameter M

Fig. 10 shows the impact of convective parameters. From the figure, it is clear that by increasing convective parameters, the dimensionless surface temperature enhances.

Fig. 11 shows the variation of power-law index n. from the figure, it is clear that by increasing n parameters, the dimensionless surface temperature increases.

Fig. 12 is plotted for variation of Nusselt number agaist M It is found that the Nusselt number is reduced for various nanofluids against M parameter.

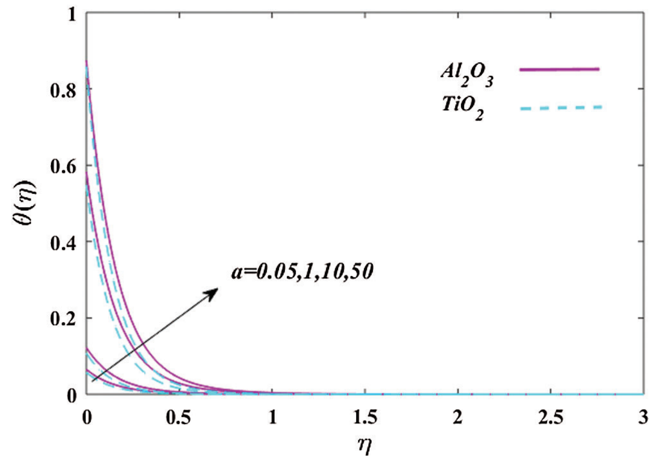

Figure 10: Effect of $\theta(\eta)$ with convective parameter a

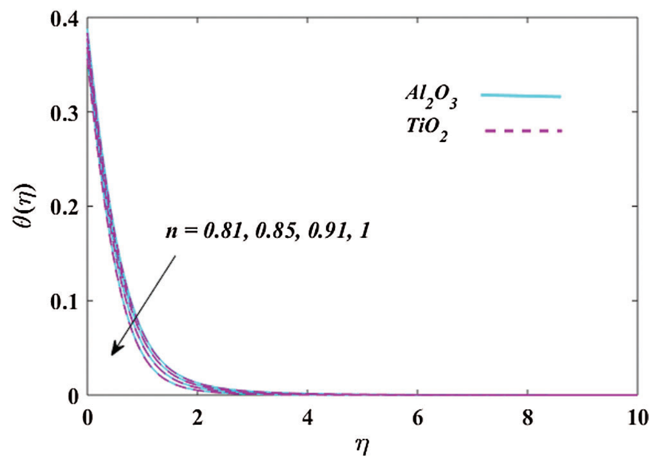

Figure 11: Effect of $\theta(\eta)$ with n

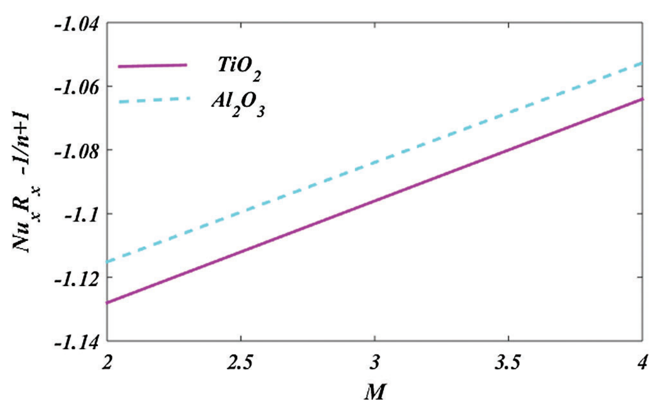

Figure 12: Effect of Nu with magnetic parameter M

Fig. 13 is drawn to show the variation of skin friction against M parameter. It is found that the skin friction number enhances with the increase of the magnetic field.

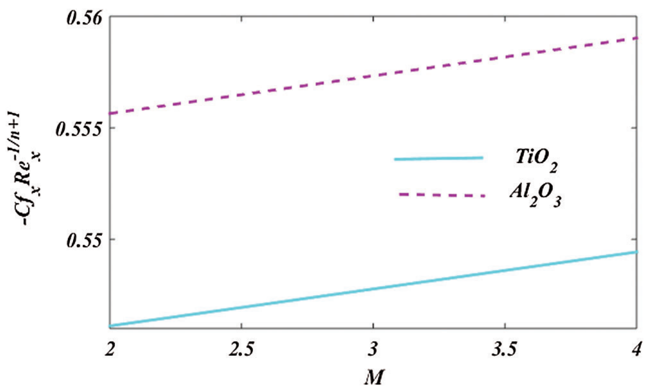

Figure 13: Effect of Cf_x with magnetic parameter M

In addition to this, the solution of partial differential equations which are governing equations of Non-Newtonian power-law fluid flow over the sheet is found using the software-based finite element method. Using the software, following kinematic viscosity is chosen for power-law fluid

$\mu = \eta (\gamma)^{m-1}$

$\gamma = \max\left(\sqrt{D\colon D}, \gamma_{\min}\right), \quad D = \frac{1}{2}\left(\Delta u + (u)^t\right).$

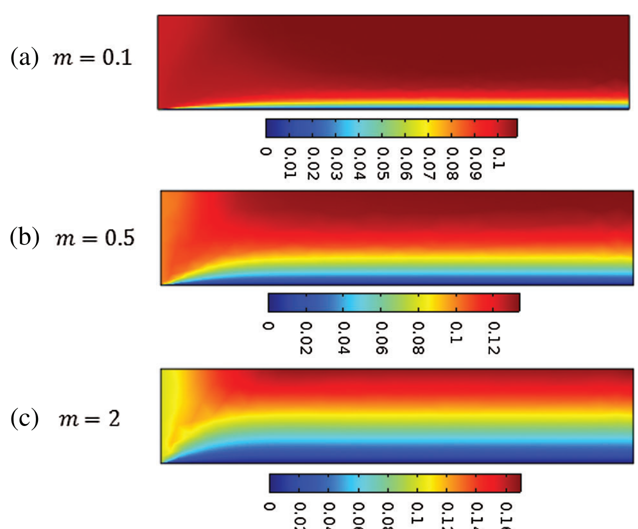

Figure 14: Surface plots of the velocity profile with $m = 0.1$, $m = 0.5$, and $m = 2$

where $\gamma_{\min} = 0.01\frac{1}{s}$ and $n = 1$. Figs. 14 and 15 show the surface plot with the variation of the parameter m. The effect of the parameter on the boundary layer and streamlines can be seen in these figures. An increase in the thickness of the boundary layer increase with the enhancement of m and corresponding streamlines can be seen in Fig. 15. Similarly, the effect of normal inflow velocity on surface plots of velocity and isothermal contours can be seen in Figs. 16 and 17. An effect of normal inflow velocity on the thermal boundary layer and corresponding isotheral contours can be seen in Figs. 15 and 16. The convective heat flux is used at the bottom wall which is given by

$-n.(-k\nabla T) = h.(T_{ext} - T)$

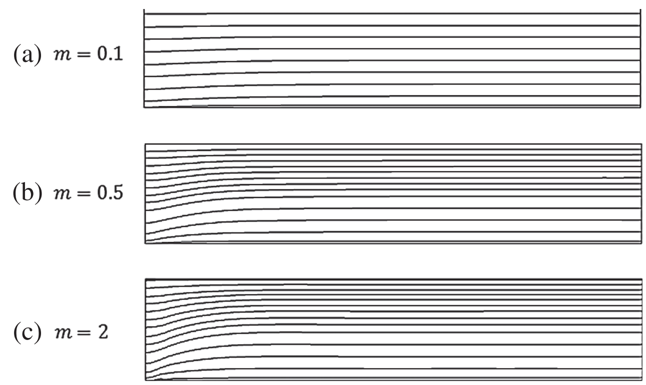

Figure 15: Plot of streamlines with $m = 0.1$, $m = 0.5$, and $m = 2$

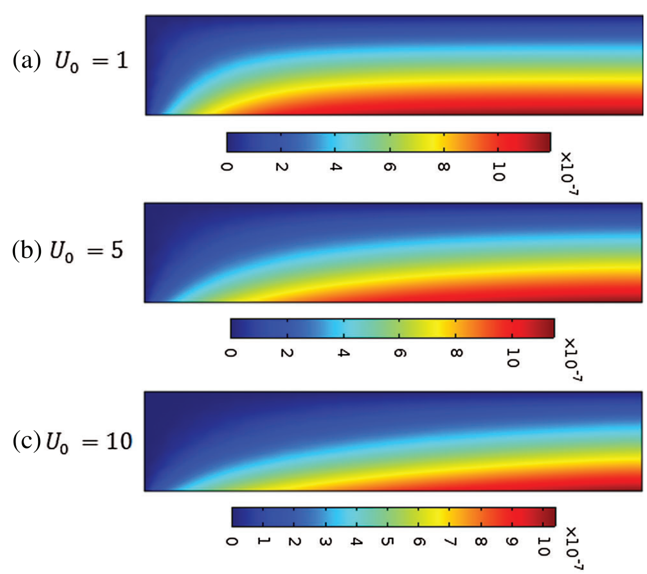

Figure 16: Surface plots of the temperature profile

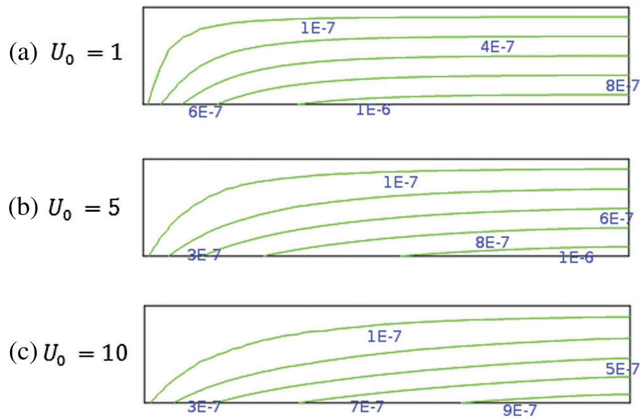

Figure 17: Isothermal contours with $U_0 = 1$, $U_0 = 5$, and $U_0 = 10$

where $h = 5$ and $T_{ext} = 1$ where T_{ext} is the temperature of the outside fluid. A Dirichlet type boundary condition for temperature is used at the top and left walls. The left wall is used as an inlet, and the right wall is used as an outlet. The normal inlet velocity is denoted by U_0. In Figs. 12–15, the power-law fluid model without considering the effects of the magnetic parameter is used instead of the nanofluid model given earlier in this work.

7 Conclusion

In this paper, we investigate the Blasius flow. We take into account the effects of the magnetic field with a power law. Moreover, we consider the Newtonian and non-Newtonian case for Blasius flow. The leading equations for the flow model are changed into non-dimensional ODEs by using appropriate similarity transformation. Then the system of ODEs is numerically solved by using the shooting method along with the R-K method. The effect of different parameters on velocity and temperature profiles for Blasius is considered. We observed some important results from our discussion, which are as follows:

- Velocity profile decreases for Blasius flow against various values of volume fraction for both cases of Newtonian and non-Newtonian fluid.
- In both cases of Newtonian and non-Newtonian fluid, the Blasius flow decreases against the velocity profile in order to reduce the value of the transpiration rate. Temperature profiles are found to be enhancing in the case of Blasius flow against the rising values of volume fraction in cases of a Newtonian fluid.
- The temperature profile increases with an increase in the Prandtl number.

Acknowledgement: We always warmly, thanks to anonymous referees. The authors are grateful to Vice-Chancellor, Air University, Islamabad for providing an excellent research environment and facilities.

Funding Statement: The fifth author also thanks Prince Sultan University for funding this work through research-group number RG-DES2017-01-17.

Conflicts of Interest: The authors declares that they have no conflicts of interest to report regarding the present study.

References

1. Zainali, A., Tofighi, N., Shadloo, M. S., Yildiz, M. (2013). Numerical investigation of Newtonian and non-Newtonian multiphase flows using ISPH method. *Computer Methods in Applied Mechanics and Engineering, 254,* 99–113. DOI 10.1016/j.cma.2012.10.005.
2. Sui, J., Zheng, L., Zhang, X., Chen, G. (2015). Mixed convection heat transfer in power law fluids over a moving conveyor along an inclined plate. *International Journal of Heat and Mass Transfer, 85,* 1023–1033. DOI 10.1016/j.ijheatmasstransfer.2015.02.014.
3. Jalil, M., Asghar, S. (2013). The flow of power-law fluid over a stretching surface: A lie group analysis. *International Journal of Non-linear Mechanics, 48,* 65–71. DOI 10.1016/j.ijnonlinmec.2012.07.004.
4. Patil, P., Roy, S., Chamkha, A. J. (2010). Mixed convection flow over a vertical power-law stretching sheet. *International Journal of Numerical Methods for Heat & Fluid Flow, 20(4),* 445–458.
5. Suresh, K., Kannan, A. (2011). Effects of particle diameter and position on hydrodynamics around a confined sphere. *Industrial & Engineering Chemistry Research, 50(23),* 13137–13160. DOI 10.1021/ie2000852.
6. Choi, S. U., Eastman, J. A. (1995). Enhancing thermal conductivity of fluids with nanoparticles. Argonne National Lab. https://www.osti.gov/biblio/196525-enhancing-thermal-conductivity-fluids-nanoparticles.
7. Jha, B. K., Samaila, A. K., Ajibade, A. O. (2013). Unsteady/steady natural convection flow of reactive viscous fluid in a vertical annulus. *International Journal of Applied Mechanics and Engineering, 18(1),* 73–83. DOI 10.2478/ijame-2013-0005.
8. Mahmoud, M. A. A. (2011). Slip velocity effect on a non-Newtonian power-law fluid over a moving permeable surface with heat generation. *Mathematical and Computer Modelling, 54(5–6),* 1228–1237. DOI 10.1016/j.mcm.2011.03.034.
9. Godson, L., Raja, B., Mohan Lal, D., Wongwises, S. (2010). Enhancement of heat transfer using nanofluids an overview. *Renewable and Sustainable Energy Reviews, 14(2),* 629–641. DOI 10.1016/j.rser.2009.10.004.
10. Lin, Y., Zheng, L., Zhang, X. (2014). Radiation effects on Marangoni convection flow and heat transfer in pseudo-plastic non-Newtonian nanofluids with variable thermal conductivity. *International Journal of Heat and Mass Transfer, 77,* 708–716. DOI 10.1016/j.ijheatmasstransfer.2014.06.028.
11. Ramesh, G., Chamkha, A. J., Gireesha, B. (2014). Magnetohydrodynamic flow of a non-Newtonian nanofluid over an impermeable surface with heat generation/absorption. *Journal of Nanofluids, 3(1),* 78–84. DOI 10.1166/jon.2014.1082.
12. Madhu, M., Kishan, N., Chamkha, A. (2016). Boundary layer flow and heat transfer of a non-Newtonian nanofluid over a non-linearly stretching sheet. *International Journal of Numerical Methods for Heat & Fluid Flow, 26(7),* 2198–2217. DOI 10.1108/HFF-02-2015-0066.
13. Yazdi, M., Hashim, I., Sopian, K. (2014). Slip boundary layer flow of a power-law fluid over moving permeable surface with viscous dissipation and prescribed surface temperature. *International Review of Mechanical Engineering, 8(3),* 502–510.
14. Dai, Y. J., Zhang, H. F. (2004). Numerical simulation and theoretical analysis of heat and mass transfer in a cross flow liquid desiccant air dehumidifier packed with honeycomb paper. *Energy Conversion and Management, 45(9–10),* 1343–1356. DOI 10.1016/j.enconman.2003.09.006.
15. Ahmed, A., Siddique, J., Sagheer, M. (2018). Dual solutions in a boundary layer flow of a power law fluid over a moving permeable flat plate with thermal radiation, viscous dissipation and heat generation/absorption. *Fluids, 3(1),* 1–6. DOI 10.3390/fluids3010006.
16. Gupta, A. S., Misra, J. C., Reza, M. (2003). Effects of suction or blowing on the velocity and temperature distribution in the flow past a porous flat plate of a power-law fluid. *Fluid Dynamics Research, 32(6),* 283–294. DOI 10.1016/S0169-5983(03)00068-6.
17. Alfvén, H. (1942). Existence of electromagnetic-hydrodynamic waves. *Nature, 150(3805),* 405–406.
18. Narsu, S., Kumar, R. B. (2018). Comparative study of chemically reacting Blasius and Sakiadis unsteady MHD radiated flow with variable conductivity. *Journal of Physics Conferences, 1000,* 1–14.

19. Krishna, C. M., ViswanathaReddy, G., Souayeh, B., Raju, C. S. K., Rahimi-Gorji, M. et al. (2019). Thermal convection of MHD Blasius and Sakiadis flow with thermal convective conditions and variable properties. *Microsystem Technologies, 25(10),* 3735–3746. DOI 10.1007/s00542-019-04353-y.
20. Chen, C. H. (1999). Forced convection over a continuous sheet with suction or injection moving in a flowing fluid. *Acta Mechanica, 138(1–2),* 1–11. DOI 10.1007/BF01179537.
21. Mahmoud, M. A. A. (2011). Slip velocity effect on a non-Newtonian power-law fluid over a moving permeable surface with heat generation. *Mathematical and Computer Modelling, 54(5–6),* 1228–1237. DOI 10.1016/j.mcm.2011.03.034.
22. Tiwari, R. K., Das, M. K. (2007). Heat transfer augmentation in a two-sided lid-driven differentially heated square cavity utilizing nanofluids. *International Journal of Heat and Mass Transfer, 50(9–10),* 2002–2018. DOI 10.1016/j.ijheatmasstransfer.2006.09.034.
23. Arif, M. S., Nawaz, Y., Bibi, M., Ali, Z. (2018). Mass transfer of MHD nanofluid in presence of chemical reaction on a permeable rotating disk with convective boundaries, using Buongiorno's Model. *Computer Modeling in Engineering & Sciences, 116(1),* 31–49. DOI 10.31614/cmes.2018.00434.
24. Maleki, H., Safaei, M. R., Alrashed, A. A. A. A., Kasaeian, A. (2019). Flow and heat transfer in non-Newtonian nanofluids over porous surfaces. *Journal of Thermal Analysis and Calorimetry, 135(3),* 1655–1666. DOI 10.1007/s10973-018-7277-9.
25. Mustafa, M., Khan, J. A., Hayat, T., Alsaedi, A. (2018). Numerical solutions for radiative heat transfer in ferrofluid flow due to a rotating disk: Tiwari and Das model. *International Journal of Nonlinear Sciences and Numerical Simulation, 19(1),* 1–10. DOI 10.1515/ijnsns-2015-0196.
26. Umavathi, J. C., Hemavathi, K. (2019). Flow and heat transfer of composite porous medium saturated with nanofluid. *Propulsion and Power Research, 8(2),* 173–181. DOI 10.1016/j.jppr.2019.01.010.
27. Anjali Devi, S. P., Suriyakumar, P. (2018). Effect of magnetic field on Blasius and Sakiadis flow of nanofluids past an inclined plate. *Journal of Taibah University for Science, 11(6),* 1275–1288. DOI 10.1016/j.jtusci.2017.03.004.
28. Mahanthesh, B., Gireesha, B. J., Gorla, R. S. R. (2016). Heat and mass transfer effects on the mixed convective flow of chemically reacting nanofluid past a moving/stationary vertical plate. *Alexandria Engineering Journal, 55(1),* 569–581. DOI 10.1016/j.aej.2016.01.022.
29. Oztop, H. F., Abu-Nada, E. (2008). Numerical study of natural convection in partially heated rectangular enclosures filled with nanofluids. *International Journal of Heat & Fluid Flow, 29(5),* 1326–1336. DOI 10.1016/j.ijheatfluidflow.2008.04.009.